Sains Malaysiana 45(4)(2016): 633–641

# Study and Characterisation of the Post Processing Ageing of Sago Pith Waste Biocomposites

(Kajian dan Pencirian Penuaan Pasca Pemprosesan Biokomposit Hampas Empulur Sagu)

JAU CHOY LAI*, WAN AIZAN WAN ABDUL RAHMAN, LUC AVÉROUS & TECK HOCK LIM

ABSTRACT

*This paper reports the post-processing ageing phenomena of thermoplastic sago starch (TPS) and plasticised sago pith waste (SPW), which were processed using twin-screw extrusion and compression moulding techniques. Wide angle X-ray diffraction (XRD) analyses showed that after processing, starch molecules rearranged into $V_H$-type (which was formed rapidly right post processing and concluded within 4 days) and B-type (which was formed slowly over a period of months) crystallites. Evidence from Fourier transform infrared spectroscopy (FTIR) analyses corroborated the 2-stage crystallisation process, which observed changes in peak styles and peak intensities (at 1043 and 1026 $cm^{-1}$) and band-narrowing. Thermogravimetric analysis (TGA) studies showed that the thermal stability of plasticised SPW declined continuously for 90 days before gradual increments ensued. For all formulations tested, post-processing ageing led to drastic changes in the tensile strength (increased) and elongation at break (decreased). Glycerol and fibres restrained the retrogradation of starch molecules in TPS and SPW.*

*Keywords: Retrogradation; sago pith waste; thermoplastic starch; thermal degradation; tensile properties*

ABSTRAK

*Kertas ini melaporkan fenomena penuaan pasca pemprosesan kanji sagu termoplastik (TPS) dan hampas empulur sagu memplastik (SPW) yang diproses menggunakan teknik penyemperitan skru berkembar dan pengacuan mampatan. Analisis pembelauan sinar-X (XRD) menunjukkan bahawa selepas pemprosesan, molekul kanji disusun semula ke dalam hablur jenis $V_H$ (berlaku dengan cepat selepas pemprosesan dan selesai dalam tempoh 4 hari) dan jenis B (berlaku secara perlahan dalam tempoh beberapa bulan). Bukti daripada analisis transformasi Fourier inframerah (FTIR) menyokong proses penghabluran 2-peringkat, yang menunjukkan perubahan dalam gaya dan keamatan puncak (pada 1043 dan 1026 $cm^{-1}$) dan jalur-penyempitan. Analisis termogravimetri (TGA) menunjukkan bahawa kestabilan haba untuk SPW terplastik menurun secara berterusan selama 90 hari sebelum kenaikan secara beransur-ansur berlaku. Untuk semua formulasi yang diuji, penuaan pasca pemprosesan membawa kepada perubahan drastik dalam kekuatan tegangan (bertambah) dan pemanjangan pada waktu rehat (menurun). Gliserol dan serat menghalang retrogradasi molekul kanji dalam TPS dan SPW.*

*Kata kunci: Hampas empulur sago memplastik; kanji termoplastik; penurunan terma; retrogradasi; sifat tegangan*

## INTRODUCTION

One of the main characteristics of thermoplastic starch (TPS)-based composites is their time-dependant behaviour during and after processing. After melt processing, the predominantly amorphous products are yet to achieve thermodynamic equilibrium. Starch chains are still mobile, even at temperatures below its glass transition temperature ($T_g$) and densification (physical ageing) may occur (Averous & Halley 2009; Champion et al. 2000). At a temperature above $T_g$, the system will evolve towards equilibrium conditions; starch macromolecules rearrange and recrystallize (retrogradation phenomenon) over time. These phenomena (physical ageing or retrogradation), which may cause changes to the structural and macroscopic properties during storage, are collectively known as post processing ageing (Averous 2004; Halley & Averous 2014). In light of the significant impact of the ageing phenomenon on the macroscopic properties, e.g. strength and flexibility of starch-based plastic products, one must understand and incorporate its effects in the phases of product design and development (Smits et al. 1999, 1998).

While there is a plethora of references on gelatinised starch or TPS retrogradation (Ambigaipalan et al. 2013; Karim et al. 2000; Schwartz et al. 2014; van Soest 1996), technical reports on TPS composites using cellulose fibres as an additive are still scarce. The bulk of the research evaluated the effects of the fibre additive on starch retrogradation and was largely devoted to food products (Goldstein et al. 2010; Lebesi & Tzia 2011; Santos et al. 2008; Yildiz et al 2013; Ronda et al. 2014). However, two studies that were based on natural fibres or microfibrils in TPS composites, did yield encouraging outcomes in that the post-processing ageing of TPS was significantly retarded through fibre-matrix interactions in a 3D-network stabilised by numerous low intermolecular bonds (Averous & Boquillon 2004; Averous et al. 2001).

This article describes our findings during the study of the post-processing ageing phenomena of TPS and plasticised sago pith waste (SPW). SPW is a starch-based system, which contains fibrous residues derived from the sago starch manufacturing process. It has been previously reported that this high starch content waste (65% starch and 35% fibre, by weight) could be successfully plasticised and processed into biocomposites through twin screw extrusion employing water and glycerol as plasticisers, thus eliminating the need for adding any plastic material (Lai et al. 2014, 2013), as previously done (Toh et al. 2011; Yee et al. 2011).

The samples were prepared from a set of multiphase systems (based on neat sago starch or pith waste) and were characterised by a range of techniques, namely, wide angle X-ray diffraction (XRD), Fourier transform infrared (FTIR), thermogravimetric analysis (TGA) and scanning electron microscopy (SEM).

## Experimental Details

### RAW MATERIALS

Sago pith waste (SPW) and sago starch (SS) were kindly provided by Ng Kia Heng Sago Industry, Johor (Malaysia). SPW has been characterised and its properties and composition (starch and moisture content and particle size distribution) were reported elsewhere (Lai et al. 2013). Regarding the handling of SPW, raw SPW from the factory was first dried under sunlight and later ground into a fine powder using a grinder. Prior to mixing with other components, SPW powder was further dried in an oven at a temperature of 105°C for 6 hours to ensure that all the moisture was removed. Glycerol from Fisher Chemicals was used as the plasticizer. Calcium stearate (CaS), purchased from Sun Ace Kakoh (M) Sdn. Bhd, was used as a processing aid. All the materials and chemicals were used directly without further purification.

### FORMULATION AND COMPOUNDING OF THE MATERIALS

Samples with pre-determined formulae were prepared according to those listed in Table 1. Distilled water and glycerol were added to aid the plasticization and extrusion of the starch and SPW. Total (distilled water + glycerol) added to SPW-G35 and SPW-G45 was 70 phr, 15 phr more comparing to TPS. This is because the formal contain fibre and thus need more processing aid in the extrusion process. For each sample, the components were mixed for 5 min using a high-speed mixer at a speed of 2000 rpm at room temperature. The mixtures were then kept in a fully sealed bag for 24 h at room temperature before plasticisation. The compounding was performed with a twin-screw extruder (Sino PSM30 B5B25 - Sino Alloy Machinery Inc.) with a screw diameter of 32 mm and 10 heating zones. The compounding process was carried out at a speed of 250 rpm and the extruder temperature profile was 95/95/100/90 /90/90/90/90/100/105°C. The extrudate was then pelletized and stored in a controlled chamber.

### PREPARATION OF SAMPLES

The materials were moulded into sheets, each of dimension 160 (length) × 160 (width) × 1 (thickness) $mm^3$ via compression moulding at 120°C and 13 MPa for 5 min. Prior to the application of pressure, the granules were pre-heated for 8 min, at the same temperature. The moulded samples were cooled rapidly using water right after the 5 min moulding process. The samples required for different testing were cut from the compression-moulded sheets according to the standard requirements. All samples were then stored in a controlled chamber containing a saturated solution of magnesium nitrate in order to obtain a 54% relative humidity at room temperature. Samples were taken out for various testing immediately after compression moulding and at intervals of after 4, 33, 60 and 90 days of conditioning. Additional data (after 300 days of ageing) were taken using XRD and TGA as supporting data.

## Characterisation of the Starch-Based Materials

### TENSILE TEST

The tensile strength and elongation at break of the moulded samples were determined using a Lloyd Tensile Machine (USA). The dimensions of the test specimens conform to the Type V sample of the ASTM D638-03. The test was carried out at a crosshead speed of 1 mm/min. On average, six samples were tested for each formulation.

### SCANNING ELECTRON MICROSCOPY

A JEOL JSM-6390LV Scanning Electron Microscope operated at 15 kV and secondary electron imaging (SEI) mode was used to examine the morphology of the tensile

TABLE 1. Formulations for plasticised SPW

| Formulation | Wt% | | phr | | |
|---|---|---|---|---|---|
| | SPW | SS | Water | Glycerol | CaS |
| TPS | 0 | 100 | 20 | 35 | 2 |
| SPW-G35 | 100 | 0 | 35 | 35 | 2 |
| SPW-G45 | 100 | 0 | 25 | 45 | 2 |

*phr = parts per hundred parts of resin

fractured surface of the specimens. Representative samples were mounted on conductive carbon tapes adhered to aluminium stubs and were subsequently coated with gold under a vacuum using a JEOL JFC-1600 Auto-Fine Coater to prevent charging during imaging and analysis.

### THERMOGRAVIMETRIC ANALYSIS

An accurately weighted sample (in the range of 10 mg) was loaded in a platinum pan. Analyses were conducted using a Perkin Elmer TGA 7 analyser at a temperature range of 30-700°C, a heating rate of 20°C/min and a nitrogen purging rate of 20 mL/min.

### WIDE-ANGLE X-RAY DIFFRACTION

Wide angle X-Ray diffraction (XRD) was employed to study the morphological properties of the plasticised SPW using a Siemens D5000 diffractometer (Germany) equipped with a copper anode X-ray tube and Cu-Kα radiation (wavelength: 1.5406 Å) at room temperature. The range of scans was $2\Theta$ = 5°-40° at the speed of 0.03° per 2 seconds. The same sample from each formulation was used for this test throughout the whole ageing period.

### FOURIER TRANSFORM INFRA-RED SPECTROSCOPY

Attenuated total reflectance-Fourier transform infrared (ATR-FTIR) studies in the range of 4000-700 $cm^{-1}$ were conducted on samples using a Perkin Elmer System 2000 FTIR spectrometer. For each spectrum, 128 scans were registered. The same sample from each formulation was used for this test throughout the whole ageing period.

## RESULTS AND DISCUSSION

The freshly compression moulded TPS samples were highly flexible and homogenous but not fully transparent. With a $T_g$ lower than the ambient temperature, the main post-processing mechanism, which took place in the samples was expected to be retrogradation and recrystallization (Averous 2004).

### CRYSTALLINITY

The XRD patterns assignment to raw SS materials has been previously reported elsewhere (Lai et al. 2013). In this study, SS was found to adopt a C-type structure (Figure 1), which agreed with the literature findings (Ahmad & Williams 1999; Pukkahuta & Varavinit 2007).

In TPS, the initial C-type structure of SS was disrupted by the twin-screw extrusion process, leading to a predominantly amorphous structure immediately after compression moulding (Figure 1). The virtually amorphous structure of TPS after processing was manifested in the form of a featureless XRD pattern, in contrast to that of raw SS. However, two broad features centred at 2θ circa 13° and 20° in the diffractogram of TPS ('After Processing', Figure 1), may be attributed to the evolving $V_H$-type crystallites ascribed to the presence of amylose-lipid complexes. These complexes formed when the linear component of SS, namely, amylose reacted with the native lipids present in SS, under the effects of thermal and mechanical forces (van Soest 1996). The complexes recrystallized rapidly into $V_H$-type crystallites, even during the cooling step of the compression moulding process.

By comparing the four sets of XRD patterns in Figure 1, one may infer that the recrystallization of the amylose-lipid complexes subsided 4 days after processing. No significant differences could be detected between the diffractograms of the samples on day-4 and day-90, specifically those signals attributed to $V_H$-type crystallites. This agrees well with the findings reported by Pushpadass and Hanna (2009) in that for TPS made from cornstarch, the most significant change in the $V_H$ crystallite peaks occurred within the first three days

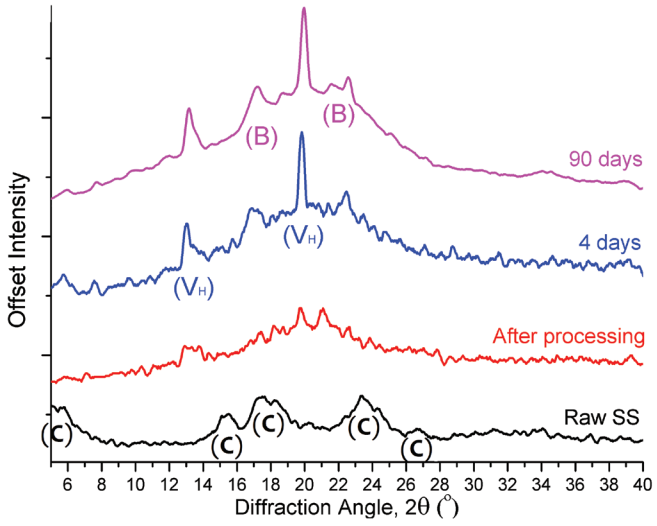


FIGURE 1. XRD diffractograms of raw SS and TPS at different points of ageing

after processing. Similar results were also reported by van Soest (1996) in his study on the ageing behaviour of potato starch-based TPS. In fact, he claimed that the crystallisation of these complexes came to completion a few hours after processing.

Four days after processing, a B-type crystalline structure (see peaks at 2θ = 17° and 22.5° Figure 1) started to emerge. The retrogradation of amylose and amylopectin is believed to be responsible for the emergence of these two peaks in two separate stages. Firstly, residue native amylose, which did not form complexes with lipids, rearranged into B-type crystallites upon cooling; this process was fast and came to completion within a few days thus, constituted most of the B-type crystallites detected on day four. On the other hand, the rearrangement of amylopectin into B-type crystallites took place at a relatively slow pace in a timespan of weeks before it concluded. This gradual growth of B-type crystallites from amylopectin later led to sharper and better-formed peaks at 2θ of 17° and 22.5° on day 90.

The retrogradation of plasticised SPW closely follows the trend found in TPS, as described in the last paragraph. $V_H$-type crystallites were detected shortly after processing and no significant changes in diffractograms were observed as time passed (Figure 2). In contrast, as the sample aged during storage, B-type crystallites became more noticeable (with its evolvement commencing on day-4 after processing), as evidenced by the more intense and sharper correspondent peaks at 2θ = 17° and 22.5°.

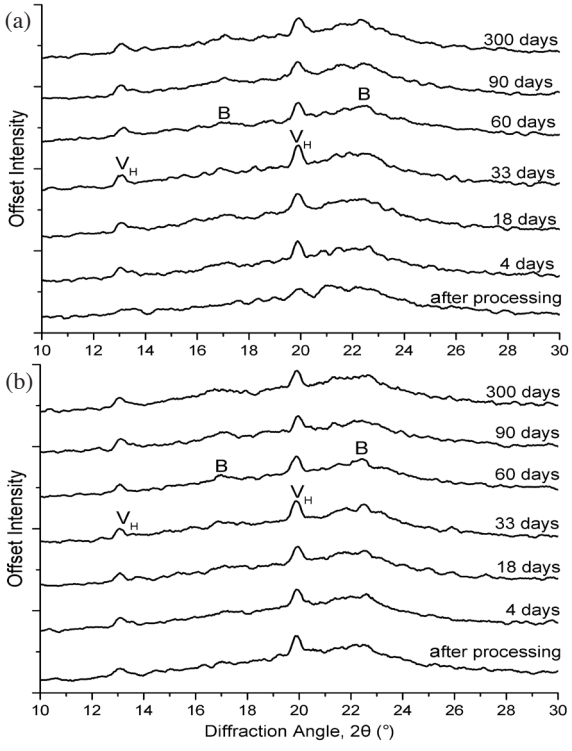


FIGURE 2. XRD Diffractograms of (a) SPW-G35 and (b) SPW-G45 at different ageing times

FOURIER TRANSFORM INFRA-RED SPECTROSCOPY

In Figure 3, band narrowing in the FTIR spectra of SPWs (as processed and after ageing) was observed. The narrowing could be attributed to the retrogradation of plasticised SPWs, as cited in a report by Goodfellow and Wilson (1990), in which pea amylose and waxy maize amylopectin were examined.

In the FTIR spectrum of the sample after processing, no distinct peaks were identified. As the samples aged, several peaks (at 1043, 1026 and 994 $cm^{-1}$) became more prominent with sharper and better formed peaks (see spectra labelled as the 60 days for SPW-G35 and 90 days for SPW-G45). The origin of the change has previously been identified to be the rearrangement of starch molecules (Pushpadass & Hanna 2009). The peaks located at 1043 and 1026 $cm^{-1}$ are sensitive to crystallinity while those centred at 994 $cm^{-1}$ vary in response to a change in the moisture content of the sample (van Soest et al. 1995).

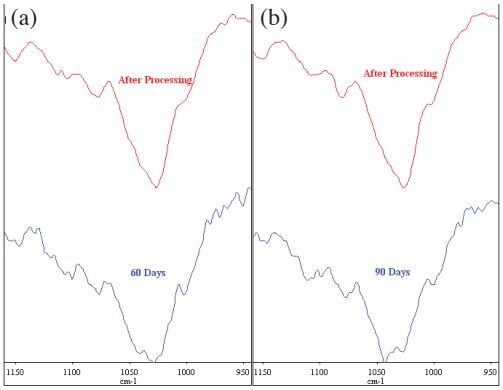


FIGURE 3. FTIR spectrums of (a) SPW-G35 and (b) SPW-G45 before and after ageing

Right after processing, the peak at around 1026 $cm^{-1}$ is evident, which corresponds to the amorphous starch hot gel systems (van Soest et al. 1994). This peak subsided as the crystallinity of ageing samples improved (signified by the growth of a peak at 1043 $cm^{-1}$) over a period of 60 days (SPW-G35) and 90 days (SPW-G45) (Pushpadass & Hanna 2009). These observations corroborated the inference previously extracted from XRD analysis.

TENSILE TEST

The evolutions of tensile strength and elongation at break of TPS and the plasticised SPW G35 and G45 within 90 days of the ageing period are captured in Figure 4. It is apparent that ageing has induced drastic changes to the tensile properties of all the tested materials, specifically within the first 33 days. As discussed, ageing took place within the first four days, during which the retrogradation of native amylose promoted an increment in tensile strength of 144, 5228 and 27% for TPS, SPW-G35 and SPW-G45, respectively. However, their elongation at break points suffered a drop of 89, 20 and 41%.

As the recrystallization of amylopectin (B-type crystallite formation) ensued, further enhancement in tensile strength was observed for all three materials. Relative to the data on day-4, the tensile strength of TPS, SPW-G35 and SPW-G45 further increased to 2296, 11 and 3935%, respectively, within a month. This is consistent with van Soest's observation (van Soest 1996) in which the retrogradation of amylopectin (B-type crystallites formation) was found to be liable for the changes observed in the mechanical properties of thermoplastic potato starch on a long-term basis.

A further question arises: How did the retrogradation process lead to the changes in the mechanical properties of these composites? Pushpadass and Hanna (2009) offered an explanation: A reinforced starch network took form due to an intermolecular crystallisation process involving the physical cross-linking between the amylopectin and amylose-amylopectin chains, whose formation led to an improved tensile strength at the expense of a decrement in flexibility.

After 33 days of ageing, the recrystallization process ceased, reaching a plateau after which the values of tensile properties only fluctuated within a small range. This behaviour was the result of a decreasing mobility of amylopectin chains as the crystallinity of the material was improving with time (Pushpadass & Hanna 2009). At the end of the 90-day ageing, the tensile strength of TPS, SPW-G35 and SPW-G45 increased by 7100, 5800 and 5000%, respectively, at the expense of the 90, 50 and 50% drop in their elongation at break point.

From the data provided, four remarks may be made:

The most notable improvement in tensile strength is that of SPW-G35 after 4 days of ageing, which indicated that the retrogradation process in this formulation commenced earlier compared to SPW-G45, owing to its lower glycerol content, which exerted lesser resistance to the rearrangement of amylopectin molecules into B-type crystallites.

The retrogradation rate (obtained from the percentage of tensile strength increment over time) of TPS was appreciably higher over those of plasticised SPW. We asserted that the fibres present in SPW were the major contributor to this phenomenon inasmuch as its presence reduced the mobility of amylopectin molecules, and, thus, hindered its recrystallization process.

The difference observed between the two plasticised SPWs was attributed to their different glycerol content; the higher the glycerol content, the lower the retrogradation rate and extent. Once again, it echoed the previous studies by other researchers (van Soest et al. 1996). At this point, a conclusion can be drawn from these observations, i.e. glycerol and fibre can serve as the agent to restrain the rearrangement of amylopectin molecules hence, reduce the effects of post-processing ageing on the mechanical properties of starch-based plastics.

The glycerol content in SPW exerts a significant effect on its ability to withstand tensile stress along with the ageing strengthening phenomenon. A 10% decrease from 45% to 35% glycerol resulted in an increase in tensile strength (Figure 4(a)). This is in accordance with the findings of Pushpadass and Hanna (2009) in that the same trend was observed for plasticised cornstarch. They attributed the effect to an increased free volume and weakened interactions between the starch chains in the starch-fibre composite network. However, the flexibility of the samples did not show considerable change when the glycerol content was varied.

The effects of post-processing ageing were also apparent from the SEM micrographs, as shown in Figure 5. The surface of the tensile-fractured TPS samples after compression moulding displayed a ductile behaviour, and the event of plastic deformation was clearly inferred by the presence of a fibrillated structure. When subjected to tensile stress, TPS was being pulled out and drawn into fibrils whose form contributed to the extremely high elongation at break value of TPS at this point of time.

After 33-days, the fibrillated structure was replaced by scale-like markings as shown in Figure 5(b) and 5(c), believed to be connected to the plastic deformation and stress whitening of TPS (Chaléat 2008). The existence of smooth regions amongst the scale-like markings signalled

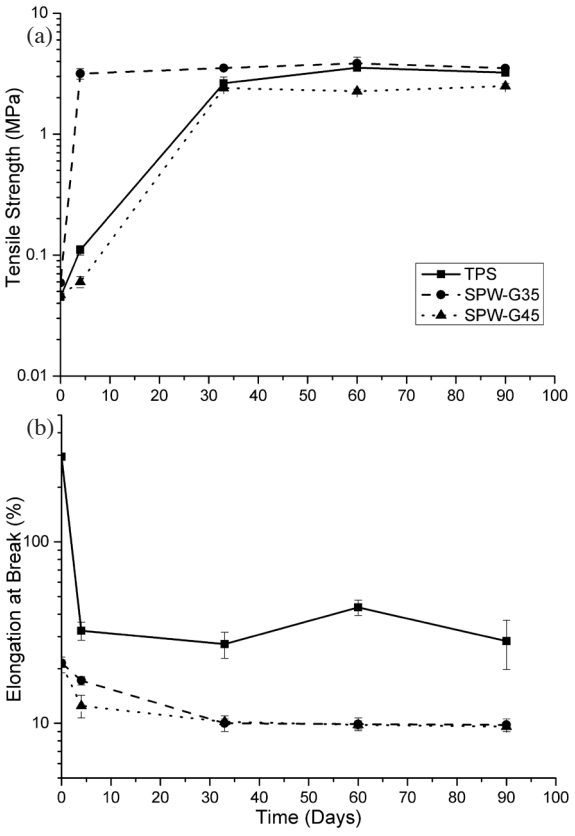


FIGURE 4. Evolution of (a) Tensile strength and (b) Elongation at break of TPS and plasticised SPW within 90 days of ageing

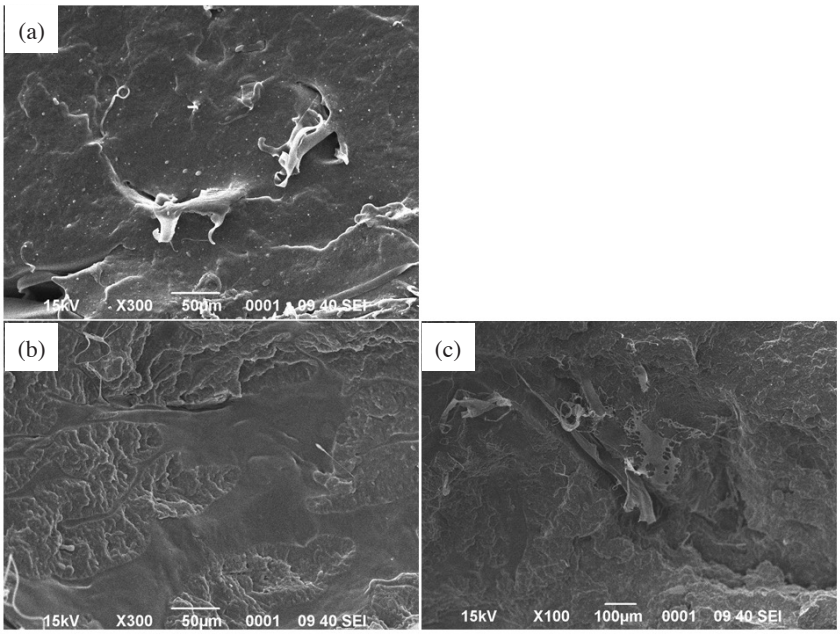


FIGURE 5. SEM micrograph of TPS (a) After compression moulding and (b) After 33 days of ageing. Fibrils formed from the pulling of largely amorphous TPS after compression moulding. Structural changes from fibrils to scale-like occurred, which is attributable to the formation of VH and B type crystallites upon ageing

the occurrence of brittle fracture and residual flexibility in TPS. The previous discussions based on XRD and tensile test results were once again validated.

## THERMAL RESISTANCE

Mass loss derivative curves of SPW-G35 and SPW-G45 are presented in Figure 6(a) and Figure 6(b), respectively. Details of thermal degradation of every individual component which constituted the composites, including TPS and SPW had been discussed in details in a separate publication (Lai et al. 2013) and will not be discussed here. It is clearly shown in the figure that, an unprecedented trend is evident that the major degradation range (MGR) and the temperature at the peak degradation rate of the two SPWs formulated were at their maxima after processing. Later, these values decreased with increasing ageing time and reached their minima on the 90th day, after which increasing time saw the increment in these values until the 300th day.

As shown in Table 2, the two plasticised SPWs behaved similarly in terms of the changes involving the two thermal degradation parameters (namely, the major degradation range (MGR) and the temperature at the peak degradation rate) as a function of ageing time. For instance, the temperature at the peak degradation rate on the 90th day is 309°C for both SPW-G35 and SPW-G45. Since, in the range of MGR, both glycerol and water would have been boiled off from the system completely, it made sense to exclude them in the explanation of the new trend in both SPWs. The most logical cause leading to the different thermal resistance behaviour lies with the components of fibre present in the two plasticised SPWs. It is known that fibre addition to TPS may significantly modify the qualitative and quantitative thermal profiles of starch gelatinisation and the kinetics of amylopectin retrogradation (during storage), although the extent of the modification is dependent on the source of the fibre (Rosell & Santos 2010).

Santos et al. (2008) found that the dietary fibre added to the bread could physically interfere with the amylopectin

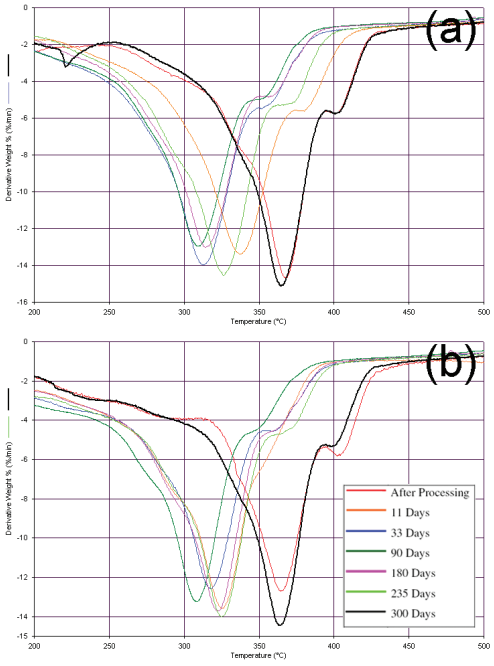


FIGURE 6. Derivative mass loss curve at different ageing days for (a) SPW-G35 and (b) SPW-G45

TABLE 2. Thermal degradation analysis of TPS and plasticised SPW

| Formulation (Day) | Major degradation range (MGR) | Weight loss in MGR | Peak degradation rate in MGR | Temperature at the peak degradation rate |
|---|---|---|---|---|
| | °C | % | %/min | °C |
| SPW-G35 (0) | 312 - 430 | 47 | 15 | 368 |
| SPW-G35 (11) | 275 - 417 | 39 | 13 | 338 |
| SPW-G35 (33) | 245 – 390 | 51 | 14 | 313 |
| SPW-G35 (90) | 252 – 390 | 45 | 13 | 309 |
| SPW-G35 (180) | 258 – 394 | 45 | 13 | 314 |
| SPW-G35 (235) | 261 - 407 | 53 | 15 | 326 |
| SPW-G35 (300) | 310 – 426 | 50 | 15 | 365 |
| SPW-G45 (0) | 315 – 430 | 43 | 13 | 366 |
| SPW-G45 (11) | 269 - 400 | 44 | 14 | 325 |
| SPW-G45 (33) | 255 – 395 | 44 | 13 | 318 |
| SPW-G45 (90) | 241 – 390 | 46 | 13 | 309 |
| SPW-G45 (180) | 255 – 395 | 47 | 14 | 322 |
| SPW-G45 (235) | 270 - 405 | 47 | 14 | 325 |
| SPW-G45 (300) | 306 – 428 | 48 | 14 | 364 |

recrystallization process, retarding the kinetics of retrogradation. Additionally, the hydrophilic nature of the fibre facilitated a starch-fibre interaction, locking down and reducing the amount of starch available for further crystallisation. This, in turn, led to the formation of less perfect crystallites resulting in a lower melting temperature and a broader endothermic transition. As hydrophilic fibre also interacts with the water present in TPS, a reduction in the availability of free water molecules helps restrain the retrogradation process (Bárcenas & Rosell 2007).

However, the underlying mechanism, which leads to the observed trends in the kinetics of retrogradation, remains unclear at this point of time and further research is required. Nevertheless, our results clearly demonstrate that adding fibre to TPS changes the retrogradation behaviour of the system and makes the material significantly better and versatile. Moreover, we envisage that our work reported herein would aid in broadening the application range of TGA in TPS related research.

## CONCLUSION

The post-processing ageing phenomena of plasticised SS and SPW were reported. The samples were examined and characterised using a range of methods inclusive of XRD, FTIR, TGA, tensile test and SEM. The changes at the molecular level and their manifestation in the properties of the materials are discussed:

From the XRD analysis, starch molecules rearranged into $V_H$-type and B-type crystallites after processing with the former developing rapidly and concluding within 4 days, and the latter proceeding slowly over a period of months. The changes observed in FTIR spectra correlated to the emergence of crystallinity from the initially amorphous starch hot gel after processing. These changes include a band-narrowing, evolvement of peak shapes and varied peak intensities within the range 1150-950 $cm^{-1}$, specifically, two registered at 1043 and 1026 $cm^{-1}$. Upon ageing, molecular restructuring takes place in TPS and plasticised SPW, which are reflected in the bulk properties leading to an increase in the tensile strength and a decline in elongation at break in all the formulations tested. The TGA analysis showed that the thermal stability of the plasticised SPWs follows a trend with two-stages: it receded first, and, upon reaching the 90th day maturity, a gradual increment took place. Glycerol and fibre were identified as the two compounds that restrained the retrogradation process of TPS.

Concerning the thermal resistance of plasticised SPWs, an unprecedented ageing trend was observed, providing fresh insights into the effect of the addition of fibre on the retrogradation of TPS and its thermal stability. Thus, the authors propose that TGA is a useful tool in studying the retrogradation of fibre filled TPS.

The rapid changes occurred in starch-based plastics, specifically their strength and flexibility after-processing, which restricts their potential and development into successful consumer products. To capitalise on the unique properties of starch-based plastics, it is imperative that one learns to control the post-processing ageing in starch plastic materials in order to guarantee the applicability of this environmentally friendly material in the movement of replacing and reducing the use of non-biodegradable plastic materials. A holistic approach must be taken in the design of starch-plastic based products, integrating the production process of starch-plastics and the post-production control of starch retrogradation phenomena. To which, the mechanical properties of the starch based plastics and products should be considered only after the retrogradation process has reached maturity.

## ACKNOWLEDGEMENTS

This work has been financially supported by the Fundamental Research Grant Scheme (Grant Number 4F289) and Research University Grant Scheme (Grant

Number 05H89) provided by the Ministry of Education (MOE), Malaysia and Universiti Teknologi Malaysia, respectively; for which the authors express their gratitude.

REFERENCES

Ahmad, F.B. & Williams, P.A. 1999. Effect of salts on the gelatinization and rheological properties of sago starch. *Journal of Agricultural and Food Chemistry* 47: 3359-3366.

Ambigaipalan, P., Hoover, R., Donner, E. & Liu, Q. 2013. Retrogradation characteristics of pulse starches. *Food Research International* 54: 203-212.

Avérous, L. & Halley, P.J. 2009. Biocomposites based on plasticized starch. *Biofuels, Bioproducts and Biorefining* 3: 329-343.

Avérous, L. 2004. Biodegradable multiphase systems based on plasticized starch: A review. *Journal of Macromolecular Science - Polymer Reviews* 44: 231-274.

Averous, L. & Boquillon, N. 2004. Biocomposites based on plasticized starch: Thermal and mechanical behaviours. *Carbohydrate Polymers* 56: 111-122.

Avérous, L., Fringant, C. & Moro, L. 2001. Plasticized starch-cellulose interactions in polysaccharide composites. *Polymer* 42: 6565-6572.

Bárcenas, M.E. & Rosell, C.M. 2007. Different approaches for increasing the shelf life of partially baked bread: Low temperatures and hydrocolloid addition. *Food Chemistry* 100: 1594-1601.

Chaléat, C. 2008. Structure-property relationships of plasticised starch/poly(vivyl alcohol) blends. PhD, University of Queensland, Australia (Unpublished).

Champion, D., Le Meste, M. & Simatos, D. 2000. Towards an improved understanding of glass transition and relaxations in foods: Molecular mobility in the glass transition range. *Trends in Food Science & Technology* 11: 41-55.

Goldstein, A., Ashrafi, L. & Seetharaman, K. 2010. Effects of cellulosic fibre on physical and rheological properties of starch, gluten and wheat flour. *International Journal of Food Science & Technology* 45: 1641-1646.

Goodfellow, B.J. & Wilson, R.H. 1990. A fourier transform IR study of the gelation of amylose and amylopectin. *Biopolymers* 30: 1183-1189.

Halley, P.J. & Averous, L. 2014. *Starch Polymers: From Genetic Engineering to Green Applications*. 1st ed. Burlington, MA: Elsevier Limited Publication.

Karim, A.Abd., Norziah, M.H. & Seow, C.C. 2000. Methods for the study of starch retrogradation. *Food Chemistry* 71: 9-36.

Lai, J.C., Rahman, W.A.W.A. & Toh, W.Y. 2014. Mechanical, thermal and water absorption properties of plasticised sago pith waste. *Fibers and Polymers* 15: 971-978.

Lai, J.C., Rahman, W.A.W.A. & Toh, W.Y. 2013. Characterisation of sago pith waste and its composites. *Industrial Crops and Products* 45: 319-326.

Lebesi, D.M. & Tzia, C. 2011. Staling of cereal bran enriched cakes and the effect of an endoxylanase enzyme on the physicochemical and sensorial characteristics. *Journal of Food Science* 76: S380-S387.

Pukkahuta, C. & Varavinit, S. 2007. Structural transformation of sago starch by heat-moisture and osmotic-pressure treatment. *Starch/Staerke* 59: 624-631.

Pushpadass, H.A. & Hanna, M.A. 2009. Age-induced changes in the microstructure and selected properties of extruded starch films plasticized with glycerol and stearic acid. *Industrial & Engineering Chemistry Research* 48: 8457-8463.

Ronda, F., Quilez, J., Pando, V. & Roos, Y.H. 2014. Fermentation time and fiber effects on recrystallization of starch components and staling of bread from frozen part-baked bread. *Journal of Food Engineering* 131: 116-123.

Rosell, C.M. & Santos, E. 2010. Impact of fibers on physical characteristics of fresh and staled bake off bread. *Journal of Food Engineering* 98: 273-281.

Santos, E., Rosell, C.M. & Collar, C. 2008. Gelatinization and retrogradation kinetics of high-fiber wheat flour blends: A calorimetric approach. *Cereal Chemistry* 85: 455-463.

Schwartz, J.M., Le Bail, K., Garnier, C., Llamas, G., Queveau, D., Pontoire, B., Srzednicki, G. & Le Bail, P. 2014. Available water in konjac glucomannan–starch mixtures. Influence on the gelatinization, retrogradation and complexation properties of two starches. *Food Hydrocolloids* 41: 71-78.

Smits, A.L.M., Hulleman, S.H.D., van Soest, J.J.G., Feil, H. & Vliegenthart, J.F.G. 1999. The influence of polyols on the molecular organization in starch-based plastics. *Polymers for Advanced Technologies* 10: 570-573.

Smits, A.L.M., Ruhnau, F.C., Vliegenthart, J.F.G. & van Soest, J.J.G. 1998. Ageing of starch based systems as observed with FT-IR and solid state NMR spectroscopy. *Starch - Stärke* 50: 478-483.

Yee, T.W., Lai, J.C. & Rahman, W.A.W.A. 2011. Mechanical and water absorption properties of poly(vinyl alcohol)/sago pith waste biocomposites. *Journal of Composite Materials* 45: 1201-1207.

van-Soest, J.J.G. 1996. Starch Plastic: Structure-Property Relationships PhD, Universiteit Utrecht, Utrecht, Netherland (Unpublished).

van Soest, J.J.G., Hulleman, S.H.D., De Wit, D. & Vliegenthart, J.F.G. 1996. Changes in the mechanical properties of thermoplastic potato starch in relation with changes in B-type crystallinity. *Carbohydrate Polymers* 29: 225-232.

van Soest, J.J.G., Tournois, H., De Wit, D. & Vliegenthart, J.F.G. 1995. Short-range structure in (partially) crystalline potato starch determined with attenuated total reflectance Fourier-transform IR spectroscopy. *Carbohydrate Research* 279: 201-214.

van Soest, J.J.G., de Wit, D., Tournois, H. & Vliegenthart, J.F.G. 1994. The influence of glycerol on structural changes in waxy maize starch as studied by Fourier transform infra-red spectroscopy. *Polymer* 35: 4722-4727.

Toh, W.Y., Sin, L.T., Rahman, W.A.W.A. & Samad, A.A. 2011. Properties and interactions of poly(vinyl alcohol)-sago pith waste biocomposites. *Journal of Composite Materials* 45: 2199-2209.

Yildiz, Ö., Yurt, B., Baştürk, A., Toker, Ö.S., Yilmaz, M.T., Karaman, S. & Dağlıoğlu, O. 2013. Pasting properties, texture profile and stress-relaxation behavior of wheat starch/dietary fiber systems. *Food Research International* 53: 278-290.

Jau Choy Lai, Wan Aizan Wan Abdul Rahman
Biopolymer Research Group
Faculty of Chemical and Energy Engineering
Universiti Teknologi Malaysia
81310 Skudai, Johor Darul Takzim
Malaysia

Wan Aizan Wan Abdul Rahman
Centre for Composites
Universiti Teknologi Malaysia
81310 Skudai, Johor Darul Takzim
Malaysia

Luc Avérous
BioTeam/ICPEES-ECPM, UMR 7515
Université de Strasbourg
25 rue Becquerel
67087 Strasbourg, Cedex 2
France

Teck Hock Lim
Department of Physical Science
Faculty of Applied Sciences & Computing
Tunku Abdul Rahman University College
Jalan Genting Kelang, Setapak 53300 Kuala Lumpur
Malaysia

*Corresponding author; email: jclai@cheme.utm.my

Received: 8 July 2015
Accepted: 22 October 2015